

# Equivalent refractive index of a sphere with multiple spherical inclusions

Adrian Doicu and Thomas Wriedt

Institut für Werkstofftechnik, Badgasteiner Strasse 3, 28359 Bremen, Germany

E-mail: thw@iwt.uni-bremen.de

Received 30 November 2000, in final form 15 March 2001

## Abstract

In this paper we analyse the scattering by a spherical particle with multiple spherical inclusions. Our analysis is focused on the equivalence between the inhomogeneous sphere and a homogeneous sphere with an equivalent refractive index. The equivalent sphere reproduces the differential scattering cross section of the inhomogeneous sphere reasonably accurately. This equivalence is investigated for small and large size parameters of the inclusions.

**Keywords:** Inhomogeneous sphere, effective-medium theories, equivalent refractive index, T-matrix method, Monte Carlo ray tracing

## 1. Introduction

Scattering of electromagnetic waves by inhomogeneous particles is an important problem in atmospheric science, astronomy and optical particle sizing. Random dispersions of inclusions in a homogeneous host medium can be equivalently considered as effectively homogeneous after using various homogenization formalisms [1, 2]. The effective-medium theories operate with various assumptions which determine their domain of applicability. An effective refractive index is defined, which reflects some average optical properties of heterogeneous materials, i.e. the effective dielectric constant relates the average electric displacement to the average electric field. The usual derivations of effective-medium approximations, for example the Maxwell–Garnett formula, are based on electrostatic considerations of the electric field and electric displacement within the heterogeneous material [1]. It is assumed that the inclusions are much smaller than the wavelength (so that the electric dipole is the only interaction term needed to describe the scattering process) and that the interactions between the inclusions can be neglected. The size-dependent polarizability relation derived in the framework of a volume integral equation approach can be used to extend the domain of applicability of the Maxwell–Garnett formula to frequencies for which the inclusions can no longer be considered very small [1]. An alternative derivation of the classical effective-medium approximations can be obtained by imposing the requirement that the scattering amplitude vanishes in the forward direction [2, 3]. The advantage of this formulation over the electrostatic approach is the natural generalization for inclusions with high size parameters.

For high particle concentrations and large size parameters of the inclusions more complete models such as the  $T$ -matrix multiple-scattering theory [4, 5] or the quasicrystalline approximation (QCA) [6], which take into account the inclusion size, statistical correlations and multiple-scattering effect, have been elaborated. In the  $T$ -matrix multiple-scattering theory one uses the QCA and the assumption that the average exciting field propagates with a new propagation constant along the incident wave direction. The generalized Lorenz–Lorentz law is then used to obtain the corresponding dispersion relation.

The effective refractive index adequately describes the transmission through a plane-parallel layer of particles. Numerical and experimental studies demonstrate that other scattering characteristics, e.g. the differential scattering cross section (DSCS) of an inhomogeneous sphere, are correctly described if the size of the inclusions and the particle concentration are small [7, 8].

In this paper we restrict our analysis to the scattering by a sphere with multiple spherical inclusions. For this type of scatterer we introduce the concept of the equivalent refractive index. The equivalent refractive index is the refractive index of a homogeneous sphere which reproduces the DSCS of the inhomogeneous sphere with a certain accuracy. The size parameters of the homogeneous and the inhomogeneous sphere are assumed to be the same. We use the term equivalent refractive index instead of effective refractive index since their definitions are different. The strategy for determining the equivalent refractive index is as follows. We use a direct scattering model to compute the DSCS of the inhomogeneous particle. The equivalent refractive index is then obtained by solving an in-

**Table 1.** Equivalent refractive index for different volume concentrations. The parameters of the simulation are  $ka_{\text{incl}} = 0.3$ ,  $m_{r,\text{incl}} = 1.2$ ,  $m_{\text{host}} = 1.3$  and  $N = 200$ .

Volume concentration of the inclusions	0.05	0.1	0.2	0.3
Equivalent refractive index	1.3126	1.3235	1.3423	1.3621

verse problem. The direct scattering models depend on the size parameters of the inclusions and the host sphere.

## 2. Model for small size parameters

For a sufficiently large number of inclusions we may assume that the scattering problem is axisymmetric. The equivalent refractive index is computed by minimizing the residual function

$$F(m) = \int_0^\pi |\sigma_d^{\text{inhom}}(\theta) - \sigma_d^{\text{host}}(\theta, m)|^2 \sin \theta d\theta, \quad (1)$$

where  $\sigma_d^{\text{inhom}}$  and  $\sigma_d^{\text{host}}$  are the DSCSs of the inhomogeneous and the homogeneous sphere, respectively, and  $m$  is the refractive index. For the solution of the above optimization problem we use stochastic methods, i.e. an evolutionary optimization algorithm [9] and a genetic algorithm [10]. The robustness of these algorithms and their capability to overcome local minimum points are essential for the inversion process.

The direct scattering model is based on the  $T$ -matrix formalism. The transition matrix of the inhomogeneous sphere can be expressed as

$$\begin{aligned} \mathbf{T}_{\text{inhom}} = & [\mathbf{T}_{\text{host}} - \mathbf{Q}_{\text{host}}^{13} \mathbf{T}_{\text{incl}} (\mathbf{Q}_{\text{host}}^{31})^{-1}] \\ & \times [\mathbf{I} + \mathbf{Q}_{\text{host}}^{33} \mathbf{T}_{\text{incl}} (\mathbf{Q}_{\text{host}}^{31})^{-1}], \end{aligned} \quad (2)$$

where  $\mathbf{T}_{\text{host}}$  is the transition matrix of the homogeneous host sphere,  $\mathbf{T}_{\text{incl}}$  is the aggregate  $T$ -matrix of the inclusions and the matrices  $\mathbf{Q}_{\text{host}}^{ij}$  have the same significance as in [11]. The above relation reflects the advantage of the  $T$ -matrix formulation, i.e. the ‘global’ system of equations corresponding to an inhomogeneous scatterer can be solved analytically by expressing the transition matrix of the inhomogeneous scatterer in terms of the transition matrices of the host particle and the inhomogeneities. Similar relations were derived for multilayered scatterers and multiple-scattering problems [11].

In this paper the generalized recursive aggregate  $T$ -matrix algorithm [12] is used to compute the aggregate  $T$ -matrix of the inclusions. Specifically,  $P$  auxiliary concentric spheres are traced in the interior of the  $(P+1)$  sphere enclosing the particles. With  $n_p$  representing the number of particles contained between the  $(p-1)$  and the  $p$  sphere, we have  $\sum_{p=1}^N n_p = N$ , where  $N$  is the total number of particles. Assuming that the aggregate  $T$ -matrix of the particles contained inside the  $(p-1)$  sphere is known, we compute the aggregate  $T$ -matrix of the particles contained inside the  $p$  sphere by adding the  $n_p$  spheres to the problem and by treating the previous spheres as a single aggregate scatterer. Thus, at each recursive step only an  $(n_p+1)$ -scattering problem needs to be solved. Since  $n_p$  is much smaller than  $N$ , the recursive solution keeps the size of the problem manageable and reduces the computational effort. The  $T$ -matrix of an aggregate will provide a valid description for the scattered field only for regions that are outside a circumscribing sphere. In the

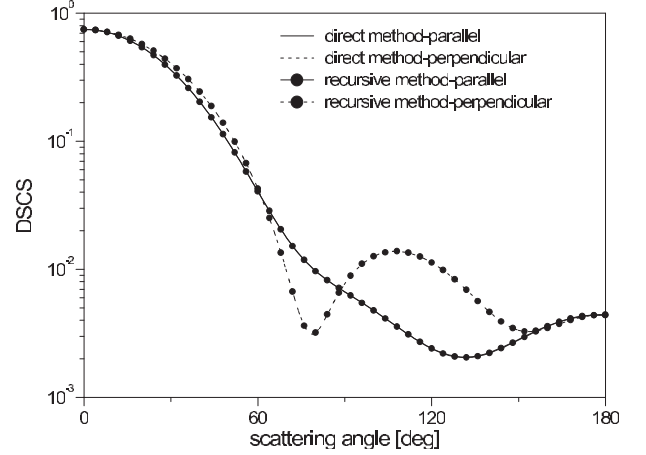


**Figure 1.** DSCS computed by using the recursive algorithm and by using the direct solution of the multiple-scattering equations.

The parameters of the simulation are  $ka_{\text{incl}} = 0.3$ ,  $m_{r,\text{incl}} = 1.2$ ,  $c = 0.2$  and  $N = 150$ . The size parameter of the host sphere is  $ka_{\text{host}} = 2.96$  and the refractive index is  $m_{\text{host}} = 1.3$ . The size parameters of the auxiliary surfaces are  $ka_1 = 2$  and  $ka_2 = 2.4$ .

process of random generation of the spheres this constraint may be violated; that is, some particles will intersect the auxiliary spheres delimiting different groups of particles. This fact questions the applicability of the recursive aggregate  $T$ -matrix algorithm. However, the simulation results plotted in figure 1 certify the accuracy of the recursive scheme. Here we plot the DSCS of an inhomogeneous sphere computed by the recursive algorithm and by the direct solution of the multiple-scattering equations. For this calculation we choose 150 spheres and a volume concentration of 0.2. The size of the inclusions is  $ka_{\text{incl}} = 0.3$  and two auxiliary concentric spheres (according to the guidelines of the recursive aggregate  $T$ -matrix algorithm) are considered in the interior of the host particle. The maximal relative error of the DSCS computed with the recursive scheme is smaller than 1%.

The random positions of particles inside the host sphere are generated by using the sequential addition method [13]. In this method the particles do not exert mutual force among themselves but they are not allowed to interpenetrate. Such non-interpenetration criteria lead to the Percus–Yevick pair distribution function for densely packed spheres. The DSCS is averaged over several configurations of the inclusions. The number of realizations is chosen such that the maximal relative error in estimating the mean DSCS is less than unity with 99% confidence.

In our simulation we consider  $N = 200$  inclusions. The volume concentration  $c$  varies between 0.05 and 0.3, while the size parameter of the inclusions  $ka_{\text{incl}}$  varies between 0.3 and 0.7. The refractive index of the host sphere is  $m_{\text{host}} = 1.3$ . Three values for the relative refractive index of the inclusions  $m_{r,\text{incl}}$  are considered: 1.2,  $1.2 + 0.35j$  and  $1.2 + 0.7j$ . The values of the equivalent refractive index we found are given

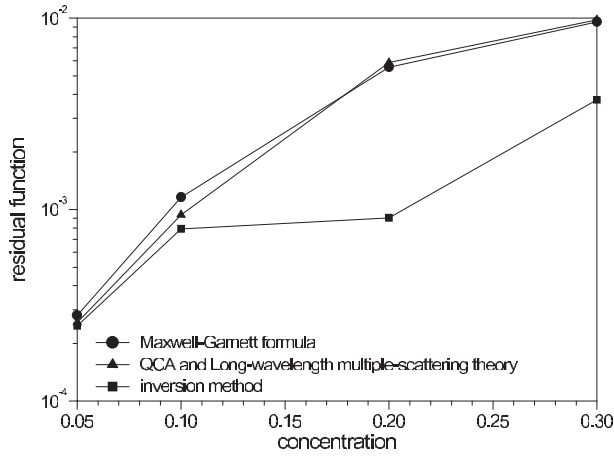


**Figure 2.** Residual function versus the volume concentration. The parameters of the simulation are  $ka_{\text{incl}} = 0.3$ ,  $m_{r,\text{incl}} = 1.2$  and  $N = 200$ . The refractive index of the host sphere is  $m_{\text{host}} = 1.3$ .

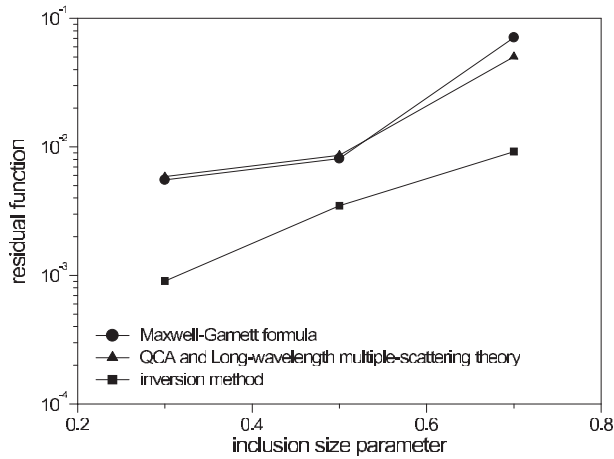


**Figure 3.** Residual function versus the size parameter of the inclusions. The parameters of the simulation are  $m_{r,\text{incl}} = 1.2$ ,  $c = 0.2$  and  $N = 200$ . The refractive index of the host sphere is  $m_{\text{host}} = 1.3$ .

**Table 2.** Equivalent refractive index for different size parameters of the inclusions. The parameters of the simulation are  $c = 0.2$ ,  $m_{r,\text{incl}} = 1.2$ ,  $m_{\text{host}} = 1.3$  and  $N = 200$ .

Size parameter of the inclusions	0.3	0.5	0.7
Equivalent refractive index	1.3423	1.3425	1.3628

in tables 1–3. We note that the evolutionary optimization algorithm and the genetic algorithm lead to the same results. In figures 2–4 we plot the minimum of the residual function together with the results obtained by using the size-dependent Maxwell–Garnett formula, the QCA and the long-wavelength  $T$ -matrix multiple-scattering theory [5]. As an example, we show in figure 5 the DSCS of the inhomogeneous and the equivalent sphere in the case  $m_{r,\text{incl}} = 1.2 + 0.7j$ . We can formulate the following concluding remarks.

(a) For non-absorbing inclusions the inversion algorithm is not able to determine accurately the imaginary part of the equivalent refractive index. Therefore, the attenuation term due to the scattering process is omitted. In fact, small values of the imaginary part of the refracted

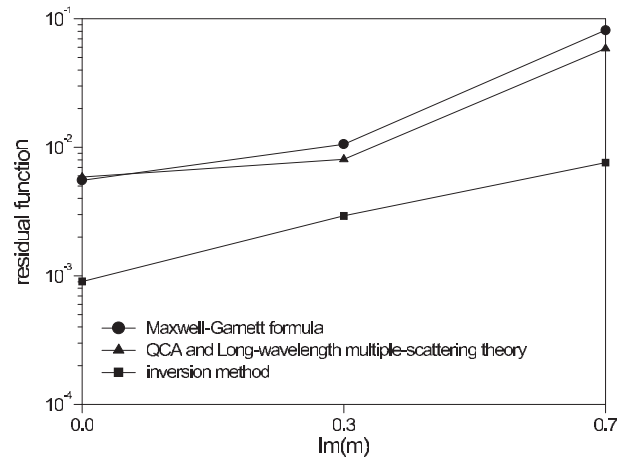


**Figure 4.** Residual function versus the refractive index of the inclusions. The parameters of the simulation are  $ka_{\text{incl}} = 0.3$ ,  $\text{Re } m_{r,\text{incl}} = 1.2$ ,  $c = 0.2$  and  $N = 200$ . The refractive index of the host sphere is  $m_{\text{host}} = 1.3$ .

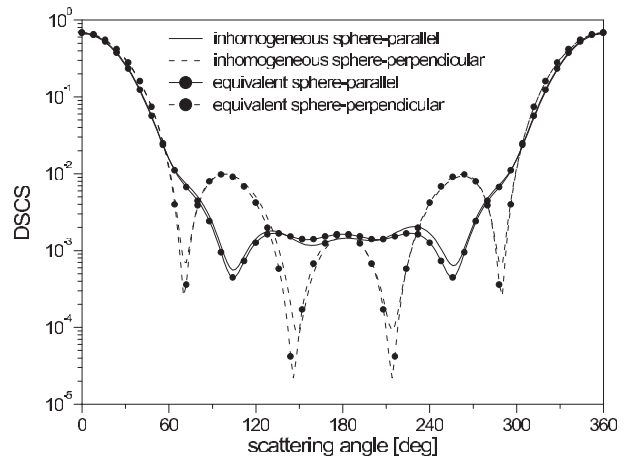


**Figure 5.** DSCS of the inhomogeneous and the equivalent sphere. The parameters of the simulation are  $ka_{\text{incl}} = 0.3$ ,  $m_{r,\text{incl}} = 1.2 + 0.7j$ ,  $c = 0.2$  and  $N = 200$ . The refractive index of the host sphere is  $m_{\text{host}} = 1.3$ .

index (as predicted by the effective-medium theories) do not influence significantly the residual function or consequently the DSCS. For instance, in the case  $ka_{\text{incl}} = 0.3$  and  $c = 0.2$  the residual function is  $F = 9.059 \times 10^{-4}$  for  $m = 1.3423$  and  $F = 9.064 \times 10^{-4}$  for  $m = 1.3423 + 5 \times 10^{-5}j$ , while in the case  $ka_{\text{incl}} = 0.5$  and  $c = 0.2$  the residual function is  $F = 3.493 \times 10^{-3}$  for  $m = 1.3425$  and  $F = 3.551 \times 10^{-3}$  for  $m = 1.3425 + 2 \times 10^{-4}j$ . These changes are smaller than the estimated precision of the numerical algorithm.

(b) The effective-medium theories provide accurate results when the size of the inclusions and the volume concentration are small and when differences in optical constants of inclusions and host particle are not too large. However, for all cases under consideration we may conclude that the QCA and the long-wavelength  $T$ -matrix multiple-scattering theory predict with sufficient accuracy the DSCS of an inhomogeneous sphere.

(c) By increasing the size of the inclusions and the volume concentration the minimum of the residual function

**Table 3.** Equivalent refractive index for different refractive indices of the inclusions. The parameters of the simulation are  $ka_{\text{incl}} = 0.3$ ,  $c = 0.2$ ,  $m_{\text{host}} = 1.3$  and  $N = 200$ .

Relative refractive index of the inclusions	1.2	$1.2 + 0.35j$	$1.2 + 0.7j$
Equivalent refractive index	1.3423	$1.3401 + 0.062j$	$1.3409 + 0.1143j$

**Table 4.** Equivalent refractive index for different volume concentrations. The parameters of the simulation are  $ka_{\text{host}} = 500$ ,  $ka_{\text{incl}} = 25$ ,  $m_{\text{host}} = 1.33$ ,  $m_{r,\text{incl}} = 1.2$ .

Volume concentration of the inclusions	0.025	0.05	0.075	0.1
Equivalent refractive index	1.48	1.58	1.67	1.80

increases. This fact questions the existence of a solution to the inverse problem, i.e. whether for any size of the inclusions and any volume concentration there exists an equivalent sphere such that the residual function is smaller than a prescribed value.

### 3. Model for large size parameters

For large size parameters of the inclusions exact scattering models are not applicable. In this context we adopt as a direct scattering model different versions of the Monte Carlo method. Since the Monte Carlo methods do not include an interference mechanism, we modify the residual function in the form

$$F(m) = \left| \int_0^{\theta_{\text{max}}} [\sigma_{\text{d}}^{\text{in hom}}(\theta) - \sigma_{\text{d}}^{\text{host}}(\theta, m)] \sin \theta \, d\theta \right|, \quad (3)$$

where  $\theta_{\text{max}}$  is the maximal value of the scattering angle for which the inversion problem is solvable.

For our simulations we use a conventional Monte Carlo method [14] and a hybrid technique combining ray optics and Monte Carlo radiative transfer [15].

In the conventional Monte Carlo method the photon starting position is randomly generated to yield either a plane wave or a Gaussian beam profile. At the point where the photon hits the host boundary we compute the Fresnel reflection coefficients  $r_s$  and  $r_p$  and compare them with an equally distributed random number within the interval  $[0, 1]$ ,  $\xi$ . If  $(r_s^2 + r_p^2)/2$  is greater than  $\xi$ , the photon is reflected. Otherwise, it is transmitted. After a photon is refracted into the host sphere, it is allowed to travel a free path length  $l = -\bar{l} \log \xi$ , where  $\bar{l}$  is the mean free path length between two subsequent scattering events. If the photon has not reached one of the boundaries, a new random number  $\xi$  is selected and two subcases arise. If  $\xi < Q_{\text{abs}}^{\text{incl}}/Q_{\text{ext}}^{\text{incl}}$  the photon is absorbed; otherwise the photon is scattered. Here,  $Q_{\text{abs}}^{\text{incl}}$  and  $Q_{\text{ext}}^{\text{incl}}$  denote the absorption and the extinction efficiencies of the inclusions. If the photon is scattered, the new scattering direction is randomly determined accordingly to the phase function of the inclusion. This procedure is repeated until the photon enters the host boundary surface, where it is again subject to reflection or refraction events.

In the hybrid model the ray-tracing procedure accounts for the individual reflection and refraction events at the boundary of the host sphere. Photons carry Mueller matrices that contribute to the ray-tracing scattering matrix. The Monte Carlo technique is used to simulate only the internal scattering process. When a scattering event occurs, the absorption is

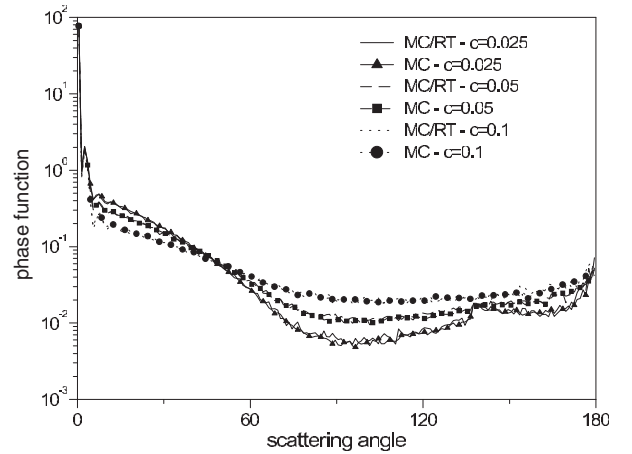


**Figure 6.** Phase functions computed with the conventional Monte Carlo method and a hybrid technique combining the Monte Carlo method and the ray tracing method. The parameters of the simulations are  $ka_{\text{host}} = 500$ ,  $ka_{\text{incl}} = 25$ ,  $m_{\text{host}} = 1.33$  and  $m_{r,\text{incl}} = 1.2$ .

taken into account by multiplying the photon energy with the single-scattering albedo of the inclusion.

In the conventional method, the number of scattered photons per unit solid angle is counted as the ray-tracing phase function. The single-scattering albedo is obtained from the ratio of the number of scattered photons to the number of incident photons. The hybrid method produces directly the ray-tracing phase function and the single-scattering albedo. Ray-tracing and diffraction properties are added and weighted by their individual scattering cross sections to obtain the total cross sections, single-scattering albedo and phase function of the inhomogeneous sphere. A comparison between the two models is shown in figure 6. Here we plot the phase function for a host sphere with a size parameter of  $ka_{\text{host}} = 500$ . The inclusions are spheres with a size parameter of  $ka_{\text{incl}} = 25$ . The refractive index of the host sphere is  $m_{\text{host}} = 1.33$ , while the relative refractive index of the inclusions is  $m_{r,\text{incl}} = 1.2$ . The results certify the accuracy of the proposed models.

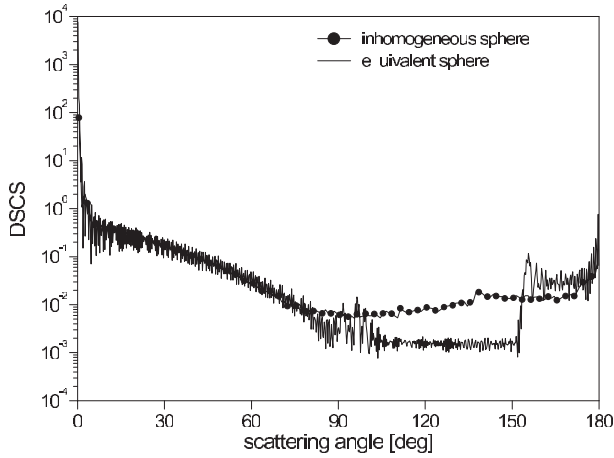
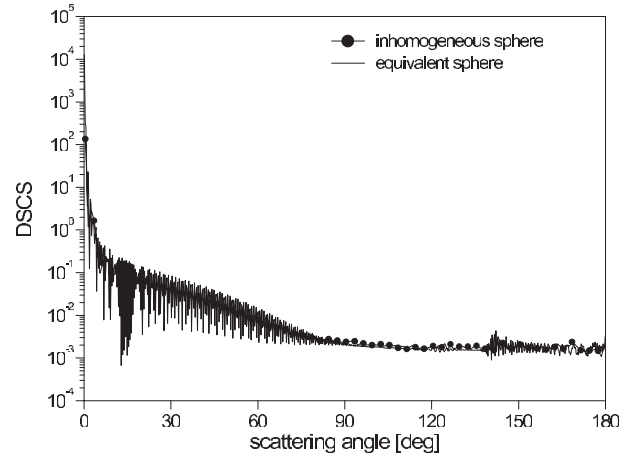
In our simulations we choose  $ka_{\text{host}} = 500$  and  $m_{\text{host}} = 1.33$ . The volume concentration varies between 0.025 and 0.1, while the size parameter of the inclusions varies between 5 and 25. Two values of the relative refractive index of the inclusions  $m_{r,\text{incl}}$  are considered: 1.2 and  $1.28 + 0.04j$ . The values of the equivalent refractive index are given in tables 4–6 together with the results obtained for highly absorbing inclusions by using the approximate formula of Sharma and Jones [16]. As examples, we plot in figures 7 and 8 the

**Table 5.** Equivalent refractive index for different size parameters of the inclusions. The parameters of the simulation are  $ka_{\text{host}} = 500$ ,  $c = 0.025$ ,  $m_{\text{host}} = 1.33$ ,  $m_{r,\text{incl}} = 1.2$ .

Size parameter of the inclusions	5	10	25
Equivalent refractive index	2.02	1.68	1.48

**Table 6.** Equivalent refractive index for different volume concentrations. The parameters of the simulation are  $ka_{\text{host}} = 500$ ,  $ka_{\text{incl}} = 25$ ,  $m_{\text{host}} = 1.33$ ,  $m_{r,\text{incl}} = 1.28 + 0.04j$ .

Volume concentration of the inclusions	0.025	0.05	0.075	0.1
Equivalent refractive index	$1.34 + 0.000385j$	$1.35 + 0.000765j$	$1.35 + 0.00112j$	$1.35 + 0.00138j$
Refractive index computed with the approximate formula	$1.33 + 0.000375j$	$1.33 + 0.000750j$	$1.33 + 0.00112j$	$1.33 + 0.00150j$

**Figure 7.** DSCS of the inhomogeneous and the equivalent sphere. The parameter of the simulations are  $ka_{\text{host}} = 500$ ,  $ka_{\text{incl}} = 25$ ,  $c = 0.025$ ,  $m_{\text{host}} = 1.33$ ,  $m_{r,\text{incl}} = 1.2$ .**Figure 8.** DSCS of the inhomogeneous and the equivalent sphere. The parameter of the simulations are  $ka_{\text{host}} = 500$ ,  $ka_{\text{incl}} = 25$ ,  $c = 0.1$ ,  $m_{\text{host}} = 1.33$ ,  $m_{r,\text{incl}} = 1.28 + 0.04j$ .

DSCS of the inhomogeneous and the equivalent sphere. The conclusions of our analysis can be summarized as follows.

- For non-absorbing inclusions the inverse problem cannot be solved over the entire scattering domain. Acceptable results can be obtained by restricting the analysis to the forward-scattering hemisphere, that is by taking  $\theta_{\text{max}} = \pi/2$ . However, even in this domain of analysis the residual function does not have a deep, distinctive minimum. The modifications of the residual function are small over a large domain of variation of the refractive index.
- For highly absorbing inclusions the inverse problem can be solved over the entire scattering domain. The agreement with the results obtained by using the approximate formula is acceptable.

#### 4. Conclusions

In this paper we introduced the concept of equivalent refractive index as the refractive index of a homogeneous sphere which accurately reproduces the DSCS of an inhomogeneous sphere. We used a direct scattering model to compute the scattering characteristics of an inhomogeneous sphere and solved an inverse problem to obtain the equivalent refractive index.

For small size parameters of the inclusions, the effective-medium theories like the QCA and the long-wavelength  $T$ -matrix multiple-scattering method provide accurate results. For large size parameters and non-absorbing inclusions the

inverse problem has acceptable solutions only in the forward-scattering hemisphere. Solutions over the complete scattering domain can be obtained only for highly absorbing inclusions.

#### Acknowledgment

We would like to acknowledge support by Deutsche Forschungsgemeinschaft.

#### References

- [1] Sihvola A 1999 *Electromagnetic Mixing Formulas and Applications* (London: Institution of Electrical Engineers)
- [2] Chýlek P and Videen G 2000 Effective medium approximations for heterogeneous particles *Light Scattering by Nonspherical Particles* ed M I Mishchenko, J W Hovenier and L D Travis (San Diego: Academic) pp 273–308
- [3] Stroud D and Pan F P 1978 Self-consistent approach to electromagnetic wave propagation and composite media: application to model granular metals *Phys. Rev. B* **17** 1602–10
- [4] Varadan V K, Brongi V N and Varadan V V 1979 Coherent electromagnetic wave propagation through randomly distributed dielectric scatterers *Phys. Rev. D* **19** 2480–9
- [5] Neo C P, Varadan V K and Varadan V V 1999 Comparison of long-wavelength  $T$ -matrix multiple-scattering theory and size-dependent Maxwell–Garnett formula *Microwave Opt. Technol. Lett.* **23** 1–4
- [6] Tsang L, Kong J A and Shin R T 1985 *Theory of Microwave Remote Sensing* (New York: Wiley)

- [7] Chýlek P and Videen G 1998 Scattering by a composite sphere and effective medium approximations *Opt. Commun.* **146** 15–20
- [8] Chýlek P, Srivastava V, Pinnick R G and Wang R T 1988 Scattering of electromagnetic waves by composite spherical particles: experiments and effective medium approximations *Appl. Opt.* **27** 2396–404
- [9] Schmiedel H 1981 Anwendung der Evolutionsoptimierung bei Mikrowellenschaltungen *Frequenz* **35** **11** 306–10
- [10] Hafner Ch and Fröhlich J 1997 Generalized Genetic Programming for Solving Engineering Problems *Proc. PIERS Symp. (Boston)* p 672
- [11] Peterson B and Ström S 1974  $T$ -matrix formulation of electromagnetic scattering from multilayered scatterers *Phys. Rev. D* **10** 2670–84
- [12] Wang Y M and Chew W C 1993 A recursive  $T$ -matrix approach for the solution of electromagnetic scattering by many spheres *IEEE Trans. Antennas Propagat.* **41** 1633–9
- [13] Ding K H, Mandt C E, Tsang L and Kong J A 1992 Monte Carlo simulations of pair distribution functions of dense discrete random media with multipole sizes of particles *J. Electromagn. Waves Appl.* **6** 1015–30
- [14] Bhandari R and Kerker M 1988 Monte Carlo analysis of the internal structure of light scattering particles with slit-scan illumination *J. Stat. Phys.* **52** 1263–83
- [15] Macke A 2000 Monte Carlo calculations of light scattering by large particles with multiple internal inclusions *Light Scattering by Nonspherical Particles* ed M I Mishchenko, J W Hovenier and L D Travis (San Diego: Academic) pp 309–22
- [16] Sharma S K and Jones A R 2000 On the validity of an approximate formula for absorption and scattering of light by a large sphere with highly absorbing inclusions *J. Phys. D: Appl. Phys.* **33** 584–8